Comparing the coherence resonance curves invoked by different types of forcing

J. Escalona, Gerardo J. Escalera Santos, and P. Parmananda
Facultad de Ciencias, UAEM, Avenida Universidad 1001, Colonia Chamilpa 62209, Cuernavaca, Morelos, Mexico
(Received 30 January 2007; revised manuscript received 20 April 2007; published 23 July 2007)

We study the different coherence resonance (CR) phenomena induced when an excitable FitzHugh-Nagumo-type system is forced using diverse deterministic and/or stochastic time series. The possible implications of this comparative study involving these different CR's are also discussed. The main result of the present work suggests that for appropriate forcing and system parameters the generated CR curves reflect the correlations of the superimposed time series.

DOI: 10.1103/PhysRevE.76.016213 PACS number(s): 05.45.−a, 82.40.Bj, 87.19.La

I. INTRODUCTION

Over the last decades tremendous interest has been generated by studies focusing on the dynamical response of excitable systems when subjected to periodic, chaotic, and/or stochastic perturbations. One of the remarkable results reported, due to its universal character, was periodic stochastic resonance (PSR) [1–5]. PSR is a resonance effect, wherein a subthreshold periodic signal is amplified with a high degree of fidelity and synchrony for an optimum value of superimposed noise. The review article [5] documents the advances made in the field of stochastic resonance and outlines the problems of current interest.

It was realized that the PSR effect persists even when noise is substituted by a chaotic signal as the nonperiodic component of the forcing signal [6]. An extension of PSR was discovered for excitable systems in which the presence of the subthreshold periodic signal was no longer necessary. Therefore, under purely stochastic perturbations the system response can exhibit enhanced regularity for an optimal noise strength. This new resonance phenomenon, named coherence resonance (CR) [7,8] was attributed to the complex interplay between the superimposed noise and the activation and excursion times intrinsic to the excitable system.

In the present work, we analyzed the CR's obtained when an excitable FitzHugh-Nagumo-type system was forced, with different types of perturbation. The superimposed perturbations employed involved time series that were purely deterministic, completely stochastic, and others which probably included both deterministic and stochastic components.

II. MODEL AND METHOD

We define our excitable system as a FitzHugh-Nagumo-(FN)-type model described by the following set of coupled nonlinear differential equations:

$$\alpha\epsilon\frac{dx}{dt} = x - \frac{x^3}{3} - y,$$

$$\alpha\frac{dy}{dt} = x + a + D\xi, \tag{1}$$

where a is the bifurcation parameter and D is the magnitude of the superimposed external perturbation ξ. In the case of purely stochastic perturbations, we considered fluctuations with Gaussian statistics i.e., a Dirac-δ-type correlation $[\langle\xi(t)\xi(t')\rangle = \delta(t-t')]$ and zero average $[\langle\xi(t)\rangle = 0]$. For all other types of perturbation (except the Lorenz time series) the following protocol was observed. The original series (χ) was translated and normalized in the following manner:

$$\xi_i = \frac{\chi_i - [\langle\chi_{max}\rangle + \langle\chi_{min}\rangle]/2}{[\langle\chi_{max}\rangle - \langle\chi_{min}\rangle]/2}, \tag{2}$$

where $\langle\chi_{max}\rangle$ and $\langle\chi_{min}\rangle$ are the averages of the maxima and the minima of the original time series. This operation (translation and normalization) ensures that ξ_i is mainly distributed in the interval $[-1,1]$, with an average of zero. Subsequently this ξ_i was superimposed on the FN system as shown in Eqs. (1).

The α parameter introduced in Eqs. (1) defines the time scale that enables the excitable system to tune in accordance with the dominant frequency (associated with the highest peak in the Fourier spectrum) of the forcing signal. This tuning of the excitable system is carried out for all the numerical calculations performed in the present work. The autonomous dynamics of the excitable FN system for $a>1$ exhibit a stable fixed point behavior. Meanwhile, for $a<1$ a stable limit cycle is observed by virtue of an underlying Hopf bifurcation at $a=1$. For values of the control parameter $a>1$, in the vicinity of the bifurcation point, the system is excitable (type II excitability). Therefore, spiking behavior can be invoked under the influence of an external stimulus if the activation threshold is crossed. The model equations (1) were integrated using the standard second-order Runge-Kutta method with a step size of $h=10^{-3}$. However, in the case of superimposed stochastic perturbations a second-order stochastic Runge-Kutta integrator [9] was used. The step size remained unchanged. The provoked coherence was quantified using the normalized variance (NV). This NV, also denoted by the symbol V_n, is calculated as $V_n = \sqrt{\mathrm{var}(t_p)}/\langle t_p\rangle$, where t_p is the time elapsed between successive spikes. Please note that both NV (abbreviation) and V_n (symbol) denote the same quantity, namely, the normalized variance.

III. RESULTS

In previous work [10], a comparative study of the CR phenomenon was carried out in an electrochemical model

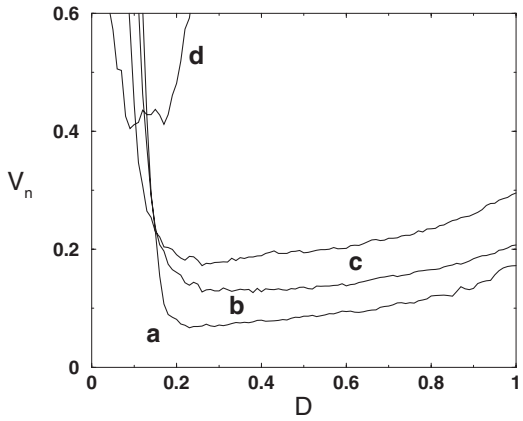

FIG. 1. Comparing the CR curve induced by Gaussian white noise (curve *d*) to the curves invoked by chaotic time series of worsening intrinsic correlations. The system parameters are $\alpha=0.071$, $\epsilon=0.01$, and $a=1.3$. The curve *a* corresponds to the CR curve provoked by the original chaotic time series (S_1); the curve *b* corresponds to the CR curve provoked by the chaotic time series with a delay of 1.0 time units (S_2). The curve *c* corresponds to the CR curve provoked by the chaotic time series with a delay of 10.0 time units (S_3). The CR curves rise as perturbations with lower correlations are employed.

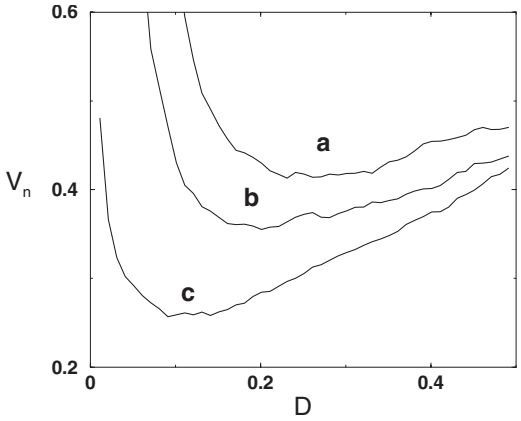

FIG. 2. Contrasting the NV curves induced by stochastic perturbations with different amplitudes of the periodic component. The system parameters are $\alpha=1.0$, $\epsilon=0.01$, and $a=1.25$. From top to bottom the NV curves correspond to (curve *a*) pure noise as the forcing signal, (curve *b*) a periodic pulse with an amplitude of 0.06, width of 1.0 time units, and a period of 2.0 time units added on the noise, and (curve *c*) a periodic pulse with an amplitude of 0.12, width of 1.0 time units, and a period of 2.0 time units, added on the noise.

[11] using chaotic signals with varying intrinsic correlations. The *z* variable of the Lorenz attractor was used as the external perturbation. In this study, as the starting point, we repeated these calculations for an excitable FN system. Chaotic time series (*z*, variable of Lorenz) of different intrinsic correlations were constructed in the following manner [10]. From the original time series (S_1) of the Lorenz *z* variable, a second time series (S_2) was generated by sampling every 1000th data point of S_1. This S_2, by design, has lower correlations than S_1. Finally, a third time series S_3 was generated by sampling every 10 000th data point of S_1. This S_3 has lower correlations than the previous time series (S_1 and S_2). These three time series with sequentially lower correlations were superimposed as ξ in Eq. (1). We observed that the loss of autocorrelation in S_3 was approximately five times faster than for S_2 and two orders of magnitude faster than for S_1.

The CR curves *a*, *b*, *c*, and *d* in Fig. 1 are invoked by the time series S_1, S_2, S_3, and a pure noise sequence, respectively. For these calculations, the model parameters were fixed at $\alpha=0.071$, $\epsilon=0.01$, and $a=1.3$. This choice ensured that the autonomous dynamics exhibited excitable fixed point behavior. Moreover, $\alpha=0.071$ tunes the excitable system dynamics to the dominant frequency of the forcing signal. These model parameters are also presented in the corresponding figure caption. It is observed that the CR curves are more elevated for perturbations with lower correlations. Consequently, the CR curve for stochastic fluctuations has the highest minima. Therefore, the maximal regularity invoked for the optimum perturbation amplitude worsens as the intrinsic correlations of the forcing time series are systematically decreased. These results indicate that the excitable system, operating in the vicinity of the bifurcation threshold, is sensitive to (able to detect) correlation variations in the superimposed forcing.

In the second set of calculations, a CR curve was computed with pure noise. Subsequently, a subthreshold periodic pulse was added to the noisy signal. Finally, the amplitude of the subthreshold periodic pulse was augmented (doubled). The curves calculated in the presence of a subthreshold signal actually correspond to the PSR curves. For these numerical simulations, the model parameters were fixed at $\alpha=1.0$, $\epsilon=0.01$, and $a=1.25$. This parameter set ensures that the autonomous dynamics exhibited excitable fixed point behavior whose intrinsic frequency is compatible with the dominant frequency of the forcing signal. Figure 2 exhibits the three V_n vs *D* curves. The system parameters are presented in the associated figure caption. The curve *a* corresponds to the scenario when the superimposed perturbation is purely stochastic. The curve *b* corresponds to the case when a small subthreshold signal is mounted on the stochastic signal. Finally, the curve *c* is found when the magnitude of the periodic component (albeit subthreshold) is doubled in the external signal. The computed curves indicate that, as the amplitude of the deterministic component in the forcing signal is increased, enhanced levels of coherence are generated. These results imply that the excitable system operating near a threshold is able to detect the variations in the magnitude of the deterministic component present in the forcing signal.

In the third phase of our work, we compared the V_n vs *D* curves provoked by different types of deterministic forcing with the CR curve for white noise. The deterministic signals employed included periodic, quasiperiodic, chaotic, and hyperchaotic time series. For this phase, the model parameters were fixed at $\alpha=0.071$, $\epsilon=0.01$, and $a=1.3$. These parameter values allow the internal frequency of the autonomous fixed point behavior to be compatible with the dominant frequency of the forcing signal. Figure 3 shows all the invoked curves in one graph. The model parameters are presented in the appropriate figure caption. Curves *e* and *d*, devoid of a uni-

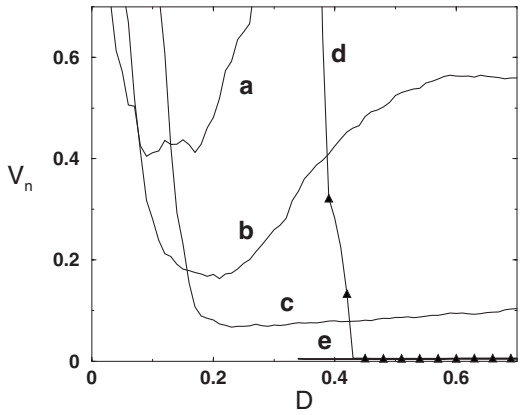

FIG. 3. Computing the NV curves for different types of deterministic forcing. The CR curve provoked by Gaussian white noise is superimposed for comparison. From top to bottom the NV curves correspond to (curve *a*) the white noise; (curve *b*) the *x* component of the four-variable Rossler system with system parameters $a=0.25$, $b=3.0$, $c=0.5$, and $d=0.05$; (curve *c*) the *z* component of the three-variable Lorenz system; (curve *d*) the quasiperiodic signal generated by $\{0.1\sin(\omega t)+0.9\sin[\sqrt{(}\pi/3)\omega t]$, with $\omega=2\pi/74.8$; (curve *e*) the periodic signal generated by $\sin(\omega t)$, with $\omega=2\pi/74.8$. The model parameters are $\alpha=0.071$, $a=1.3$, and $\epsilon=0.01$.

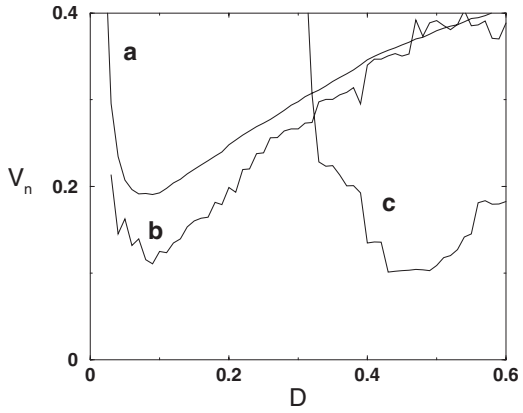

FIG. 4. NV curves for three different signals are shown, from top to bottom corresponding to (curve *a*) noise, (curve *b*) EEG, and (curve *c*) seismic. The model parameters are $\alpha=1.0$, $a=1.05$, and $\epsilon=0.01$.

modal profile (no relative minimum) correspond to periodic and quasiperiodic perturbations, respectively. Curves *c* and *b* are generated using a chaotic Lorenz signal (*z* variable) and a hyperchaotic Rossler signal (*x* variable). Finally, the curve *a* is induced by a superimposed noise. These curves indicate that (a) a CR (unimodal) curve is generated only by perturbations for which the correlations vanish asymptotically, and (b) the faster the rate of correlation decay the more elevated the CR curves, and consequently the lower the extent of the maximal regularity achieved.

Finally, the noise-provoked CR curve is compared with the NV curves induced by seismological [12] and electroencephalogram (EEG) [13] signals. The three curves are superimposed in Fig. 4. The model parameters are provided in the relevant figure caption. These three curves indicate that (a) both seismic and EEG time series have vanishing correlations manifested by the induction of unimodal CR curves; (b) both seismic and EEG signals have a higher degree of correlation than the noise, and therefore their CR curves are lower than that of noise.

IV. SUMMARY

Systematic analysis of the numerous CR curves presented in the four figures of this paper allows us to make the following conjectures.

(1) For signals with asymptotically vanishing correlations, a unimodal NV curve is generated, provided the excitable system is tuned appropriately. This inception of CR curves implies the existence of an optimum perturbation amplitude for which maximum regularity emerges.

(2) If the excitable system is tuned properly, all the generated CR curves are lower than the CR curve provoked by white noise. Moreover, as the intrinsic correlations of the superimposed perturbations worsen, the corresponding CR curves ascend. In physical terms, this implies that the extent of the maximal regularity induced is proportional to the intrinsic correlations of the perturbation signal. Since white noise is devoid of any intrinsic correlations, it defines the upper limit (lowest maximal regularity) for the induced CR curves.

The biggest challenge for the presented calculations was the appropriate tuning of the excitable system. It was realized that erroneous NV curves were generated if all the dominant frequencies of the forcing signal were not accounted for. Consequently, for forcing signals with dominant frequencies far apart, this method would fail, since the system could only be tuned (fixing α) to one of the characteristic frequencies of the perturbation signal.

Another requirement for reliable calculations is to use large time series. This enables one to attain reasonable statistics and consequently robust NV curves. However, in real situations long time series usually have problems of nonstationarity, which could impede the acquisition of reliable CR curves.

ACKNOWLEDGMENT

We are grateful to the CONACyT for support of the present work.

[1] R. Benzi, A. Sutera, and A. Vulpiani, J. Phys. A **14**, 453 (1981).
[2] R. Benzi, G. Parisi, A. Sutera, and A. Vulpiani, Tellus **34**, 10 (1982).
[3] G. Nicolis and C. Nicolis, Tellus **33**, 225 (1981); **34**, 1 (1982).
[4] S. Fauve and F. Heslot, Phys. Lett. **97A**, 5 (1983).
[5] L. Gammaitoni, P. Hanggi, P. Jung, and F. Marchesoni, Rev. Mod. Phys. **70**, 223 (1998).

[6] E. Ippen, J. Lindner, and W. Ditto, J. Stat. Phys. **70**, 437 (1993).
[7] Arkady S. Pikovsky and Jürgen Kurths, Phys. Rev. Lett. **78**, 775 (1997).
[8] G. Giacomelli, M. Giudici, S. Balle, and J. R. Tredicce, Phys. Rev. Lett. **84**, 3298 (2000).
[9] H. S. Greenside and E. Helfand, Bell Syst. Tech. J. **60**, 1927 (1981).
[10] Gerardo J. Escalera and P. Parmananda, Phys. Rev. E **65**, 067203 (2002).
[11] J. B. Talbot and R. A. Oriani, Electrochim. Acta **30**, 1277 (1985).
[12] The seismic time series was obtained as the fluctuations of the electric self-potential monitored by a dipole oriented in the north-south direction. Data were obtained from an electroseismic station on the Pacific coast through A. Ramírez-Rojas. For technical details, see A. Ramírez-Rojas, A. Muños-Diosdado, C. G. Pavia-Miller, and F. Angulo-Brown, Nat. Hazards Earth Syst. Sci. **4**, 703 (2004), and references therein.
[13] The time series correspond to an electrode channel of the EEG of a healthy subject.